1 August 2002

ELSEVIER

Optics Communications 209 (2002) 209–216

OPTICS COMMUNICATIONS

www.elsevier.com/locate/optcom

# Optical properties of Cunyite ($Cr^{4+}$ : $Ca_2GeO_4$) crystals co-doped with $Er^{3+}$ ions

M.Yu. Sharonov*, S. Owen, A.B. Bykov, W.B. Wang, R.R. Alfano

*Institute for Ultrafast Spectroscopy and Lasers, and New York State Center for Advanced Technology for Ultrafast Photonic Materials and Applications, Department of Physics, The City College and Graduate School of the City University of New York, New York, NY 10031, USA*

Received 4 December 2001; received in revised form 28 May 2002; accepted 30 May 2002

**Abstract**

The optical properties of $Cr^{4+}$ centers in $Ca_2GeO_4$ (Cunyite) single crystals co-doped with $Er^{3+}$ ions have been measured. Excitation of $Cr^{4+}$ produces both $Cr^{4+}$ fluorescence centered at 1280 nm and $Er^{3+}$ fluorescence centered at 1550 nm. The cross-section of the $^4I_{13/2}$–$^4I_{15/2}Er^{3+}$ transition is estimated using Judd–Ofelt analysis to be $8 \times 10^{-21}$ cm$^2$. The quantum efficiency of the energy transfer from $Cr^{4+}$ to $Er^{3+}$ is obtained based on measurements of the decay of fluorescence from $Cr^{4+}$. The relative populations and gain coefficients of $Cr^{4+}$ and $Er^{3+}$ centers under pumping in the $Cr^{4+}$ band are calculated with varying $Er^{3+}$ concentrations. The co-doped Cunyite ($Ca_2GeO_4$) crystal can be used as an active optical medium for 1200 to 1600 nm region. 

The demonstration of laser action in near-infrared from $Cr^{4+}$: forsterite ($Cr^{4+}$ : $Mg_2SiO_4$) by Petricevic et al. in 1988 [1] stimulated interest in the development of new lasers activated by $Cr^{4+}$ ions. Over the past several years a number of $Cr^{4+}$-based laser crystals have been grown and investigated for laser operation [2,3]. One of the few laser grade materials successfully produced by these efforts is $Cr^{4+}$ : $Ca_2GeO_4$ laser crystal called Cunyite. $Cr^{4+}$ : $Ca_2GeO_4$ has an olivine structure and is isomorphic with $Cr^{4+}$ doped forsterite but has much weaker high temperature quenching of the $Cr^{4+}$ luminescence. In contrast to forsterite, a high $Cr^{4+}$ concentration is easily achieved in the $Ca_2GeO_4$ lattice, and there is no indication of the presence of $Cr^{3+}$ [4,5]. Pulsed, cw, and passively mode-locked operation of $Cr^{4+}$ : $Ca_2GeO_4$ crystals was demonstrated with tunability in 1208–1500 nm spectral range [6,7].

In this paper, we report on the optical properties of $Ca_2GeO_4$ crystals activated by both $Cr^{4+}$ ions and $Er^{3+}$ ions. Efficient energy transfer occurs from $Cr^{4+}$ to $Er^{3+}$ ions, giving rise to $Cr^{4+}$ ions as a sensitizing agent for $Er^{3+}$ luminescence. $Cr^{4+}$ and $Er^{3+}$ can also work in emission pairs as active centers in lasers extending the tuning range of $Er^{3+}$ to the high-energy part of the spectrum (1200–1400 nm) in comparison with only $Er^{3+}$ media (1500–1650 nm).

* Corresponding author. Fax: +1-212-650-5530.
*E-mail address:* sharonov@photonicsmail.sci.ccny.cuny.edu (M.Y. Sharonov).

0030-4018/02/$ - see front matter 
PII: S0030-4018(02)01639-5

$Ca_2GeO_4$ is an olivine mineral and has Pnma $Z = 4$ space group symmetry with lattice constants $a = 11.4$ Å, $b = 6.79$ Å, $c = 5.24$ Å. $Cr^{4+}$ substitutes for $Ge^{4+}$ in a distorted tetrahedral position with site symmetry $C_s(C_{2v})$. Rare-earth ions substitute for $Ca^{2+}$ with charge compensation. Powders with 0.1, 0.25, 0.5, and 1.0 wt% of Cr were synthesized. For fluorescence decay time measurements and absorption spectra measurements good optical quality single crystals of $Er^{3+}$, $Cr^{4+} : Ca_2GeO_4$ were grown by a top-seeded solution growth method. The concentration of $Cr^{4+}$ was 0.1–1.0 wt%, and the concentration of $Er^{3+}$ was 0.5–2.0 wt%. Three samples with different polarization orientations of 0.2–2.0 mm thickness were cut for absorption measurements.

Absorption spectra were measured on a Cary 500 double beam spectrophotometer. Spontaneous emission spectra were measured upon excitation with a 680 nm laser-diode. Lifetime measurements were done upon excitation with a Q-switched Nd:YAG laser at 1064 nm wavelength with a 5 ns pulse duration and repetition frequency of ~5 Hz. The fluorescence was detected with a 20 MHz bandwidth InGaAs photodiode. Decay traces were recorded on a Tektronix TDS 684a oscilloscope and were transferred to a PC. To improve the accuracy of measurements we averaged over ~200 traces. For low-temperature measurements a Janis Research cryostat and a Lake Shore Cryotronics controller were used.

Fig. 1 shows the absorption spectra at room temperature of $Cr^{4+}, Er^{3+} : Ca_2GeO_4$ crystals for $E\|a$, $E\|b$ and $E\|c$ polarizations. The spectra consist of broadband $Cr^{4+}$ absorption (similar to absorption bands in $Cr^{4+} : Ca_2GeO_4$) and sharp lines of $Er^{3+}$ absorption. Fig. 2 shows polarized fluorescence spectra after excitation in the $^3T_1Cr^{4+}$ absorption band for 0.1 wt% $Cr^{4+}$, 1.0 wt% $Er^{3+}$ in $Ca_2GeO_4$. Broadband structureless emission centered at 1280 nm belongs to $^3T_2$–$^3A_2$ transitions of $Cr^{4+}$, and sharp lines at 1550 nm belong to $^4I_{13/2}$–$^4I_{15/2}$ transitions of $Er^{3+}$ ions. The ratio of intensities of $Er^{3+}$ and $Cr^{4+}$ fluorescence depends on the $Er^{3+}$ concentration and is determined by the efficiency of $Cr^{4+} \rightarrow Er^{3+}$ energy transfer as will be shown below.

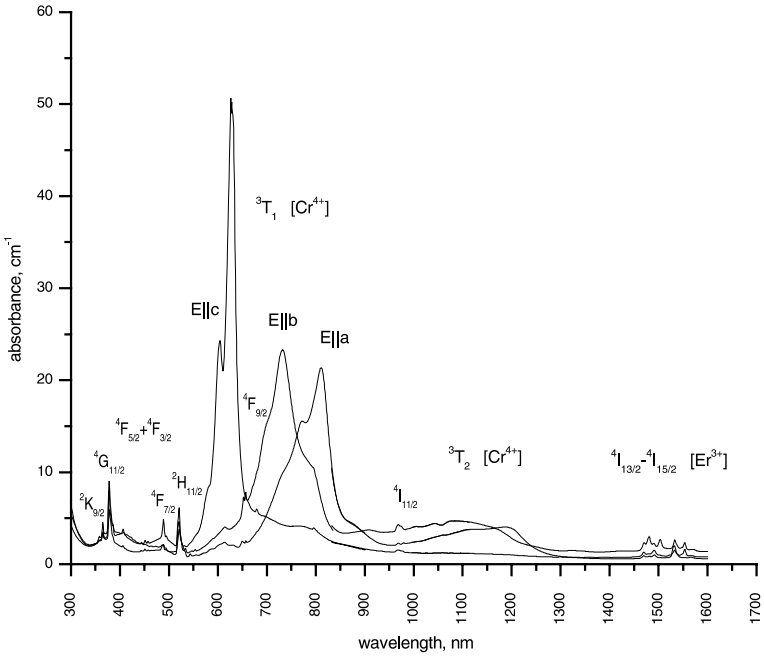


Fig. 1. Absorption spectra of (0.1 wt% $Cr^{4+}$, 1 wt% $Er^{3+}$) : $Ca_2GeO_4$ crystal for $E\|a$, $E\|b$ and $E\|c$ polarization.

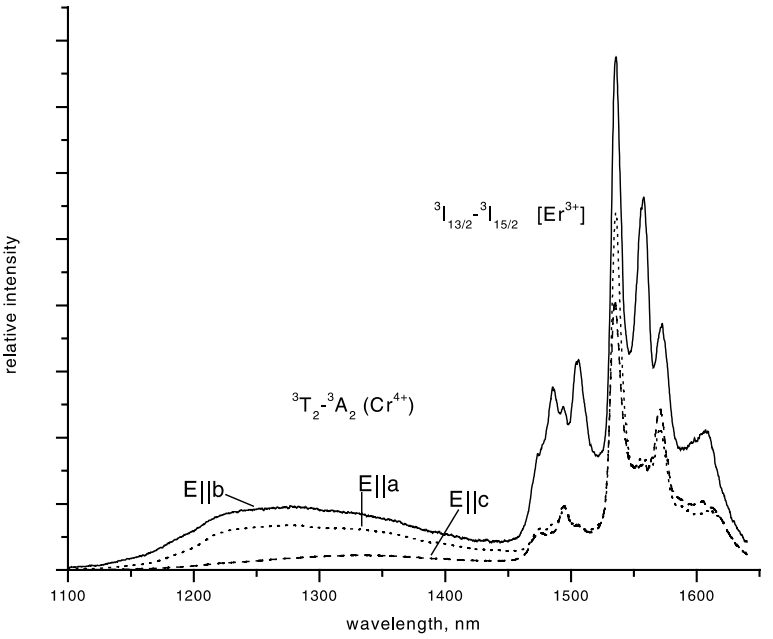


Fig. 2. Polarized fluorescence spectra upon 680 nm laser diode excitation of (0.1 wt% $Cr^{4+}$, 1.0 wt% $Er^{3+}$) : $Ca_2GeO_4$ crystals at room temperature.

The calculation of 4f–4f transition probabilities of $Er^{3+}$ ions was carried out using Judd–Ofelt theory [8,9]. Experimental line strengths were obtained from absorption spectra of $^4I_{13/2}$, $^4I_{11/2}$, $^4F_{9/2}$, $^4S_{3/2}$, $^2H_{11/2}$, $^4F_{7/2}$, $^4G_{11/2}$ and $^4G_{9/2}$ transitions using the equation

$$S^{\mathrm{ed}}_{JJ'} = \frac{\int k(\lambda)\,\mathrm{d}\lambda}{N_0} \times \frac{3ch(2J+1)}{8\pi^3 e^2 \overline{\lambda}} \times \chi, \tag{1}$$

where $\int k(\lambda)\,\mathrm{d}\lambda$ is an integrated absorption coefficient of the $JJ'$ intermanifold transition (average of all 3 polarizations), $\overline{\lambda}$ is a mean wavelength of the transition, $N_0$ is the concentration of ions, $c$ is the speed of light, $h$ is a Planck's constant, $e$ is the electron charge, and $\chi = 9\overline{n}/(\overline{n}^2+2)^2$, where $\overline{n}$ is the mean refractive index. Intensity parameters $\Omega_2$, $\Omega_4$, and $\Omega_6$ of the Judd–Ofelt theory that give the best fit with experimentally measured strengths of lines can be obtained using the matrix equation [10]

$$\overrightarrow{\Omega} = (A^{\mathrm{T}}A)^{-1}A^{\mathrm{T}}\overrightarrow{S}^{\mathrm{ed}}_{JJ'}, \tag{2}$$

where $\overrightarrow{\Omega}$ is a vector with components $\Omega_2$, $\Omega_4$, and $\Omega_6$. $A$ is a matrix composed of reduced-matrix elements determined by the experimentally measured strength of the line. $A^{\mathrm{T}}$ denotes the transposed matrix.

Calculation gives $\Omega_2 = 3.5\times10^{-20}$, $\Omega_4 = 4.3\times10^{-21}$, $\Omega_6 = 9.7\times10^{-21}$. Using the intensity parameters the spontaneous emission probability of the $^4I_{13/2}$–$^4I_{15/2}$ electronic transitions can be calculated using the equation

$$A_{JJ'} = \frac{64\pi^4 e^2 n^2}{3h(2J+1)\overline{\lambda}^3} \times \sum_{t=2,4,6} \Omega_t \left|\left\langle 4f^n S,L,J\|\|U^{(t)}\|\|4f^n S',L'J'\right\rangle\right|^2, \tag{3}$$

where $|\langle 4f^n S,L,J\|\|U^{(t)}\|\|4f^n S',L'J'\rangle|^2$ is the reduced matrix element of the $JJ'$ transition [11]. Using Eq. (3) calculation gives $A_{JJ'} = 97.4\ \mathrm{s}^{-1}$. The lifetime of the metastable level of $Er^{3+}$, using $\tau = 1/A_{JJ'}$, is 10.3 ms. This value coincides well with the experimentally measured lifetime of 9.7 ms.

The emission cross-section of the electronic transition can be found using the equation [12,13]:

$$\sigma_i = \frac{\lambda^5 A_{JJ'}}{8\pi c n^2} \frac{S_i(\lambda)}{3\sum_i \int S_i(\lambda)\lambda \, d\lambda}, \quad (4)$$

where $S_i(\lambda)$ is the intensity profile of the emission band, $i = a, b, c$ denotes the polarization. The calculated cross-sections at the maximum at 1536 nm (corresponding to the $^4I_{13/2}$–$^4I_{15/2}$ transition) for $E\|a$, $E\|b$ and $E\|c$ are $5.5 \times 10^{-21}$ cm$^{21}$, $8.0 \times 10^{-21}$ cm$^2$, and $4.5 \times 10^{-21}$ cm$^2$, respectively. The maximum emission cross-section for $Er^{3+}$ ions is $8 \times 10^{-21}$ cm$^2$, which is two orders of magnitude smaller than the maximal emission cross-section of the $Cr^{4+}$ $^3T_2$–$^3A_2$ transition, which is $8\times10^{-19}$ cm$^2$ [5].

Excitation in the $Cr^{4+}$ band with short laser pulses produces luminescence at 1170–1500 nm from $Cr^{4+}$ ions and at 1500–1650 nm from $Er^{3+}$ ions. Short-lived luminescence in the μs range is due to the $Cr^{4+}$ ions while long-lived luminescence with ~10 ms decay time is due to the $Er^{3+}$ ions. $Er^{3+}$ luminescence has a pure exponential decay with decay time 9.7 ms at room temperature and 12 ms at liquid nitrogen temperature. This decay time varies only slightly from 9.7 to 8.2 ms with $Er^{3+}$ concentration (varying within 0–2 wt% range) indicating relatively weak concentration quenching.

The luminescence lifetime of $Cr^{4+}$ in $Ca_2GeO_4$ with no $Er^{3+}$ co-doping is strongly temperature dependent and varies from ~30 μs at 77 K to ~15 μs at room temperature. The luminescence lifetime at 77 K is within a low-temperature plateau value, and the decreasing of lifetime with increasing temperature is due to nonradiative relaxation in $Cr^{4+}$ centers [4]. Therefore, we can consider the luminescence lifetime at 77 K as the radiative lifetime.

Fig. 3 shows the dependence of luminescence lifetime of $Cr^{4+}$ in $Ca_2GeO_4$ on $Cr^{4+}$ content. At low $Cr^{4+}$ concentrations (0–0.1 wt%) the quantum

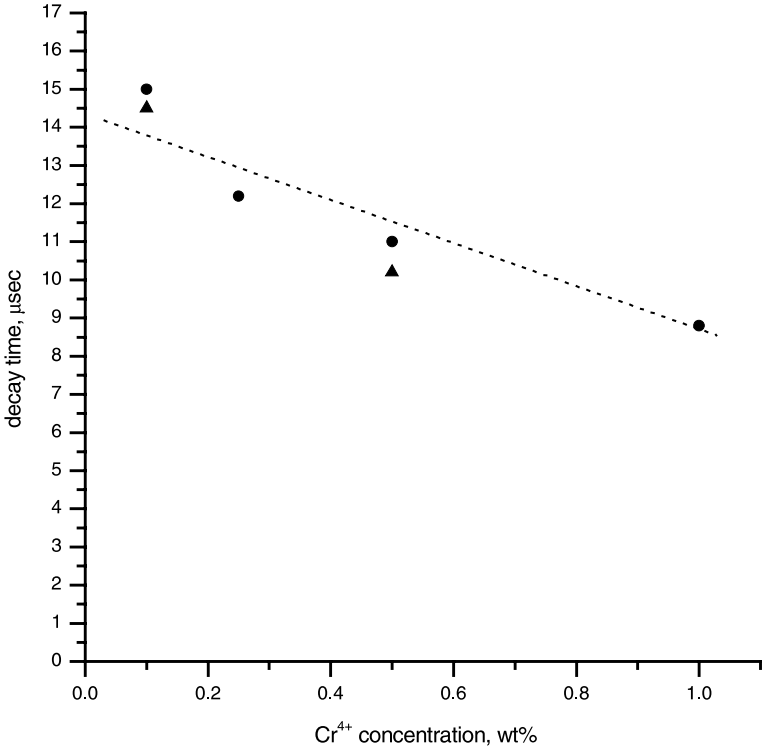


Fig. 3. Dependence of decay time of the $Cr^{4+}$ : $Ca_2GeO_4$ metastable level on $Cr^{4+}$ concentration at room-temperature. Circles represent powder samples and triangles represent single crystals.

efficiency of $Cr^{4+}$ centers, given by $\eta = \tau_{300\ K}/\tau_{77\ K}(Cr \to 0)$, is determined only by nonradiative relaxation, and is ~50%. At ~1.0 wt% concentration the quantum efficiency of $Cr^{4+}$ drops to ~30% because both of nonradiative relaxation and concentration quenching.

The decay traces of $Cr^{4+}$ fluorescence after short pulse excitation in the $^3T_2$ absorption band (1064 nm) of (0.1 wt% Cr) $Cr^{4+}:Ca_2GeO_4$ are shown in Fig. 4 at (a) 77 K and (b) 300 K; and the $Cr^{4+}$ samples are co-doped with (c) 0.5 wt% $Er^{3+}$ (d) 1.0 wt% $Er^{3+}$ and (e) 2.0 wt% $Er^{3+}$ at room temperature. When there is no $Er^{4+}$ co-doping and the $Cr^{4+}$ concentration is small the decay is close to a single exponential (shown in (a) and (b) of Fig. 4). The lifetime, $\tau_{Cr}$, is determined by

$$\frac{1}{\tau_{Cr}} = W_{rad} + W_{nrad},$$

where $W_{rad}$ is the radiative probability (inverse value of the lifetime at low temperature (30 μs)) and $W_{nrad}$ is the nonradiative probability. $\tau_{Cr}$ is equal to 30 μs at 77 K and ~15 μs at 300 K indicating nonradiative quenching of $Cr^{4+}$ luminescence. When $Er^{3+}$ ions are added to $Cr^{4+}:Ca_2GeO_4$ crystals, the decay of the $Cr^{4+}$ centers has a more complex shape and the mean lifetime is much shorter than without $Er^{3+}$.

The inter-ion energy transfer in double doped crystals is determined by (1) energy migration over donors ($Cr^{4+}$ ions), (2) energy migration between donors and acceptors ($Cr^{4+}$–$Er^{3+}$ interaction), (3) energy migration over acceptors ($Er^{3+}$ ions). Since concentration quenching of $Cr^{4+}$ and $Er^{3+}$ is relatively weak we can neglect mechanisms (1) and (3) and consider only Cr–Er energy transfer as the main mechanism of energy transfer from $Cr^{4+}$ to $Er^{3+}$.

In general temporal evolution of $Cr^{4+}$ decay can be described by [14–16]

$$I(t) = I_0 \exp\left[-\frac{t}{\tau_{Cr}} - \Pi(t)\right], \quad (5)$$

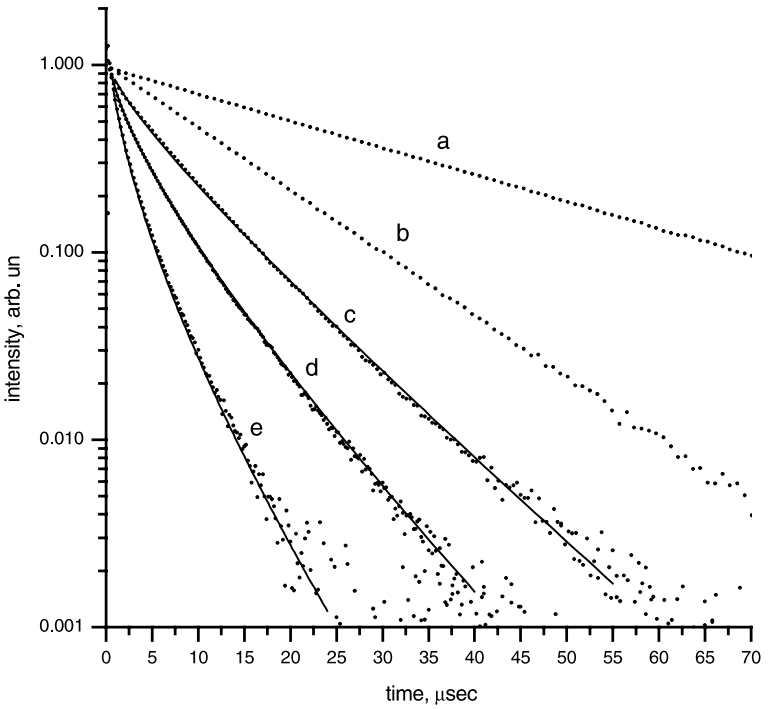


Fig. 4. Decay traces of $Cr^{4+}$ after short 1064 nm pulse excitation of (0.1 wt% $Cr^{4+}$) : $Ca_2GeO_4$ at (a) $T = 100$ K and (b) $T = 300$ K. Decay traces after short 1064 nm pulse excitation of (0.1 wt% $Cr^{4+}$) : $Ca_2GeO_4$ co-doped with (c) 0.5 wt% $Er^{3+}$, (d) 1.0 wt% $Er^{3+}$ and (e) 2.0 wt% of $Er^{3+}$ at $T = 300$ K. Solid lines show the best-fit approximation using Eq. (6).

where $\tau_{Cr}$ is the lifetime without donor–acceptor interaction, $\Pi(t)$ is function which describes $Cr^{3+}$–$Er^{3+}$ interaction.

Decays of all the studied crystals of $Cr^{4+}/Er^{3+}$ in Fig. 4 (0.1 wt% $Cr^{4+}$, 0.5, 1.0, 2.0 wt% $Er^{3+}$) can be fitted well with the equation

$$I(t) = P_1 \exp(-P_2 t - P_3\sqrt{t}), \tag{6}$$

where $P_1$, $P_2$ and $P_3$ are fitting parameters. The best fits are shown in Figs. 4(c)–(e) by solid lines. For all the studied crystals luminescence decay can be fitted with parameter $P_2$ equal to $85400 \pm 5000\ s^{-1}$; the parameter $P_3$ is proportional to the concentration of $Er^{3+}$ ions and is equal to $550 \pm 40\ s^{-1/2}\ (wt\%.)^{-1}$.

We observe that the lifetimes of $Cr^{4+}$ ions in $Cr^{4+} : Ca_2GeO_4$ crystals co-doped with rare-earth ions are slightly different from those in $Cr^{4+} : Ca_2GeO_4$ crystals with no rare-earth co-doping at 77 K (radiative lifetime) and at 300 K (determined by both nonradiative and radiative transfer). This was observed in our preliminary study of $Yb^{3+}$, $Cr^{4+}Ca_2GeO_4$ crystals where there is no energy transfer from $Cr^{4+}$ to $Yb^{3+}$. These lifetimes depend on $Yb^{3+}$ concentration and vary from 15 μs (0 wt% of Yb) to 11 μs (2 wt% of Yb) at room temperature and from 30 μs (0 wt% of Yb) to 25 μs (2 wt% of Yb) at 77 K. Such behavior may be due to a change in the refractive index of the lattice by the rare-earth ions. We will not discuss this dependence here and will assume that the radiative lifetime is 25 μs and that the room-temperature lifetime of $Cr^{4+}$ is 12 μs (hypothetical lifetime in the absence of Cr–Er energy transfer) for all the crystals with $Cr^{4+}$ concentration of 0.1 wt% and $Er^{3+}$ concentration within 0–2.5 wt%. This assumption is within the accuracy of the calculations.

Taking into account the above-mentioned values of the lifetimes, we see that the $P_2$ fitting parameter is very close to the probability of $Cr^{4+}$ decay with no donor–acceptor interaction ($1/\tau_{Cr}$) and $\Pi(t)$ in Eq. (5) in our case is $P_3\sqrt{t}$. We can conclude that temporal evaluation of $Cr^{4+}$ decay is described by static disordered decay of Förster type [17]

$$I(t) = I_0\left(-\frac{t}{\tau_{Cr}} - \gamma\sqrt{t}\right), \tag{7}$$

where $\tau_{Cr}$ is the lifetime without donor–acceptor interaction, $W$ is the coefficient of donor energy migration, and

$$\gamma = \frac{4\pi^{3/2} n_a C_{da}^{1/2}}{3} = P_3$$

is the coefficient that characterizes the static disordered decay which is proportional to the acceptor concentration, $n_a$ is the concentration of acceptor ions and $C_{da}$ is the microparameter of donor–acceptor interaction.

Using the experimentally determined parameters of energy transfer, we can now calculate the quantum efficiency of $Cr^{4+}$ luminescence, $\eta_{Cr}$, and the quantum efficiency of $Cr^{4+} \rightarrow Er^{3+}$ energy transfer $\eta_{Cr\text{–}Er}$ [18]:

$$\eta_{Cr} = \frac{1}{\tau_{rad}} \int_0^\infty \exp\left(-\frac{t}{\tau_{Cr}} - \gamma\sqrt{t}\right) dt, \tag{8}$$

$$\eta_{Cr\text{–}Er} = 1 - \frac{1}{\tau_{Cr}} \int_0^\infty \exp\left(-\frac{t}{\tau_{Cr}} - \gamma\sqrt{t}\right) dt. \tag{9}$$

The quantum efficiency $\eta_{Er}$ is close to unity because temperature and concentration quenching of $Er^{3+}$ luminescence is small.

Fig. 5 shows $\eta_{Cr}$ and $\eta_{Cr\text{–}Er}$ quantum efficiencies versus $Er^{3+}$ content calculated using Eqs. (8) and (9) with parameters $\tau_{Cr} = 12$ μs and $\gamma = P_3 = 550\ s^{-1/2}\ (wt\%)^{-1}$ obtained experimentally.

According to the theoretical model (Eq. (7)), the quantum efficiency of energy transfer – and therefore the populations of $Cr^{4+}$ and $Er^{3+}$ (normalized to absorbed power) – should be independent of $Cr^{4+}$ concentration at low $Cr^{4+}$ concentration, where the concentration quenching of $Cr^{4+}$ can be neglected.

In the presence of donors ($Cr^{4+}$) and acceptors ($Er^{3+}$), the temporal evolution of the $Er^{3+}$ subsystem under instantaneous excitation can be obtained by solving of the following differential equation [18]:

$$\frac{dN_{Er}}{dt} = -\frac{N_{Er}}{\tau_{Er}} - \frac{N_{Cr}}{\tau_{Cr}} - \frac{dN_{Cr}}{dt}, \tag{10}$$

where $N_{Er}$ and $N_{Cr}$ are the numbers of excited Er and Cr ions. Temporal dependence of Cr decay is known (Eqs. (6) and (7)), and Eq. (10) is a linear differential equation of first order. Solving the equation with the initial conditions $N_{Cr} = N_{Cr}(0)$

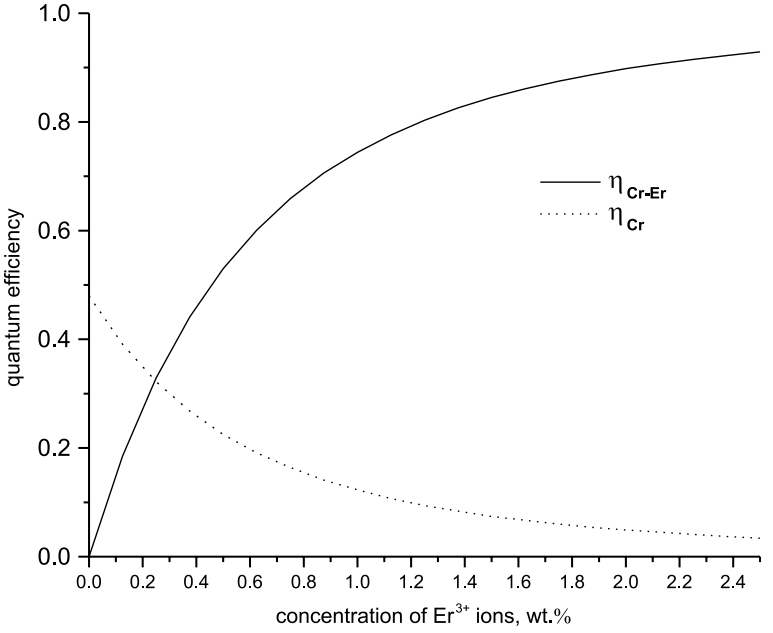


Fig. 5. Dependence of $Cr^{4+}$ quantum efficiency (dashed line) and quantum efficiency of Cr–Er energy transfer (solid line) on $Er^{3+}$ concentration.

and $N_{Er} = N_{Er}(0)$ at $t = 0$, we now obtain the temporal evolution of the Er population

$$N_{Er}(t) = N_{Er}(0)\exp\left(-\frac{t}{\tau_{Er}}\right) + N_{Cr}(0) \times \int_0^t \frac{\gamma}{2\sqrt{t'}}\exp\left(-\frac{t'}{\tau_{Cr}} - \gamma\sqrt{t'} - \frac{t-t'}{\tau_{Er}}\right)\mathrm{d}t', \tag{11}$$

where the first term is the decay of Er ions excited directly through Er absorption bands, and the second term is the time dependence of the number of excited Er ions that have received excitation through Cr ions. This temporal evolution of Er (Eq. (11)) was obtained under instantaneous excitation. For an arbitrary profile of the optical excitation pulse $\phi(t)$ it can be generalized as [18]

$$N^*_{Er}(t) = \int_0^t N_{Er}(t)\varphi(t-\tau)\,\mathrm{d}\tau. \tag{12}$$

At cw-pumping, the excited population of $Er^{3+}$ ions can be expressed using quantum efficiencies of energy transfer [18]

$$N_{Er} = P_{Er}\tau_{Er} + P_{Cr}\tau_{Er}\eta_{Cr-Er}, \tag{13}$$

where $N_{Er}$ is the excited population of $Er^{3+}$ ions, $P_{Er}$ is the power (photons/s) absorbed directly by $Er^{3+}$ absorption bands, and $P_{Cr}$ is the power of pumping absorbed by $Cr^{4+}$ absorption bands. If pumping is performed only through $Cr^{4+}$ absorption bands, the first term in Eq. (13) becomes equal to zero and the ratio of excited population of $Er^{3+}$ to $Cr^{4+}$ ions is

$$R = \frac{\tau_{Er}\eta_{Cr-Er}}{\tau_{Cr}(1-\eta_{Cr-Er})}. \tag{14}$$

Even at relatively low $Er^{3+}$ concentration, where the efficiency of Cr–Er transfer is small, the excited population of $Er^{3+}$ is much higher than the excited population of $Cr^{4+}$ because the lifetime of the $Er^{3+}$ metastable level is almost three orders of magnitude greater than the lifetime of the $Cr^{4+}$ metastable level.

The ratio of small gain coefficients of the $Er^{3+}$ and $Cr^{4+}$ bands (at 1.55 μm for $Er^{3+}$, $^4I_{13/2}$–$^4I_{15/2}$ transition, and at 1.3 μm for $Cr^{4+}$, $^3T_2$–$^3A_2$ transition) will be $(\sigma_{Er}/\sigma_{Cr})R$, where $\sigma_{Er}$ and $\sigma_{Cr}$ are the emission cross-sections and $R$ is determined by Eq. (14). To get the same gain coefficients at 1.3 and 1.55 μm, $R$ should be $\sigma_{Cr}/\sigma_{Er} = 100$ (we used

$\sigma_{Cr}$ from [5], and $\sigma_{Er}$ was determined in this paper). Using Eq. (14) we obtain $\eta_{Cr-Er} \sim 0.09$ and, using Fig. 5, the $Er^{3+}$ concentration equal to ~0.1 wt%.

In conclusion, the optical properties of $Ca_2GeO_4$ crystals co-doped with $Cr^{4+}$ ions and $Er^{3+}$ ions were investigated. The maximum emission cross-section of $Er^{3+}$ for the $^4I_{13/2}$–$^4I_{15/2}$ electronic transition is $\sim 8 \times 10^{-21}$ cm$^2$. The emission spectrum of $Ca_2GeO_4$ crystals doped with both $Cr^{4+}$ and $Er^{3+}$ consists of a $Cr^{4+}$ fluorescence band located at 1280 nm and an $Er^{3+}$ fluorescence band located at 1550 nm; the relative intensity of the bands depends on $Er^{3+}$ concentration. Pumping in the $Cr^{4+}$ absorption band populates both $Cr^{4+}$ centers and $Er^{3+}$ centers due to efficient energy transfer from the $Cr^{4+}$ ion to the $Er^{3+}$ ion. At $Er^{3+}$ concentration ~0.1 wt%, the maximum gain coefficients for the 1.3 μm $Cr^{4+}$ and the 1.55 μm $Er^{3+}$ emission bands are the same, and Cr, Er : $Ca_2GeO_4$ crystal can be used as active optical media for simultaneous operation at $Cr^{4+}$ and $Er^{3+}$ emission bands with equal gain coefficients. At $Er^{3+}$ concentration more than 2 wt%, the quantum efficiency of Cr–Er energy transfer exceeds 90%, and therefore broadband Cr absorption can be used (perfectly matching the frequency of the pump source) for effective pumping of $Er^{3+}$ ions if only $Er^{3+}$ operation is necessary.

The spectrum of the $Cr^{4+}$ : $Ca_2GeO_4$ crystals co-doped with $Er^{3+}$ matches well both the 1300 mm and 1550 nm telecommunications windows – extending the bandwidth – and may make this co-doped crystal useful as an active medium for optical communications devices in both spectral regions.

## Acknowledgements

The Army Research Office, the National Science Foundation, and the Research Foundation of the City University of New York supported this research.

## References

[1] V. Petricevic, S.K. Gayen, R.R. Alfano, K. Yamagishi, H. Anzai, Y. Yamaguchi, Appl. Phys. Lett. 52 (1988) 1040.
[2] J. Koetke, S. Kück, K. Peterman, G. Huber, G. Crullo, M. Danailov, V. Magni, L.F. Qian, O. Svelno, Opt. Commun. 101 (1993) 195.
[3] V. Petricevic, A.B. Bykov, A. Seas, R.R. Alfano, Di Yao, L.L. Isaacs, G.V. Kanunnikov, in: CLEO'97, OSA Technical Digest Series, vol. 11, 1997, p. 489.
[4] M.F. Hazenkamp, H.U. Güdel, M. Atanasov, U. Kesper, D. Reinen, Phys. Rev. B 53 (1996) 2367.
[5] V. Petricevic, A. Bykov, J.M. Evans, R.R. Alfano, Opt. Lett. 21 (1996) 1750.
[6] J.M. Evans, V. Petricevic, A.B. Bykov, R.R. Alfano, Opt. Lett. 22 (1997) 1171.
[7] Bing Xu, J.M. Evans, V. Petricevic, S.P. Guo, O. Maksimov, M.C. Tamargo, R.R. Alfano, Appl. Opt. 39 (27) (2000) 4975.
[8] B.R. Judd, Phys. Rev. 127 (1962) 750.
[9] G.S. Ofelt, J. Chem. Phys. 37 (1962) 11.
[10] W.F. Krupke, IEEE J. Quantum Electron. QE-7 (1971) 153.
[11] A. Kaminskii, Laser Crystals their Physics and Properties, Springer, Berlin, 1996.
[12] B.F. Aull, H.P. Jenssen, IEEE J. Quantum Electron. QE-18 (1982) 925.
[13] G. Huber, W.W. Kruhler, W. Bludau, H.G. Danielmeyer, J. Appl. Phys. 46 (8) (1975) 3580.
[14] Yu.K. Voronko, T.G. Mamedov, V.V. Osiko, A.M. Prokhorov, V.P. Sakun, I.A. Schrbakov, Sov. Phys. JETP 44 (2) (1976) 251.
[15] M.V. Artamonova, Ch.M. Briskina, A.I. Burshtein, L.D. Zusman, A.G. Skleznev, Sov. Phys. JETP 35 (1972) 457.
[16] I.A. Bondar, A.I. Burshtein, A.V. Krutikov, L.P. Mezentseva, V.V. Osiko, V.P. Sakun, V.A. Smirnov, I.A. Shcherbakov, Sov. Phys. JETP 54 (1) (1981) 45.
[17] Th. Förster, Ann. Phys. (Leipzig) 2 (1948) 55.
[18] V.G. Ostroumov, Yu.S. Privis, V.A. Smirnov, I.A. Scherbakov, J. Opt. Soc. Am. B 3 (1) (1986) 81.